Superlattices and Microstructures, Vol. 25, No. 5/6, 1999
Article No. spmi.1999.0744
Available online at http://www.idealibrary.com on IDEAL

General transport properties of superconducting quantum point contacts: a Green functions approach

A. MARTIN-RODERO, A. LEVY YEYATI, J. C. CUEVAS
Departamento de Física Teórica de la Materia Condensada C-V, Facultad de Ciencias, Universidad Autónoma de Madrid, E-28049 Madrid, Spain

(Received 24 March 1999)

We discuss the general transport properties of superconducting quantum point contacts. We show how these properties can be obtained from a microscopic model using nonequilibrium Green's function techniques. For the case of a one-channel contact we analyze the response under different biasing conditions: constant applied voltage, current bias and microwave-induced transport. Current fluctuations are also analyzed with particular emphasis on thermal and shot-noise. Finally, the case of superconducting transport through a resonant level is discussed. The calculated properties show a remarkable agreement with the available experimental data from atomic-size contacts measurements. We suggest the possibility of extending this comparison to several other predictions of the theory.

Key words: mesoscopic superconductivity, quantum point contacts, Andreev scattering.

1. Introduction

Since the discovery of the Josephson effect [1], the electronic transport between weakly coupled superconducting electrodes (weak superconductivity) has been a subject of growing interest [2]. Typically, weak superconductivity has been studied in SIS, SNS and S-c-S junctions, where S, N, I and c denote superconductor, normal metal, insulator and constriction, respectively. Recent technological advances have made possible the fabrication of mesoscopic S-c-S junctions in which the electrodes are connected by a small number of conduction channels. These systems are usually referred to as superconducting quantum point contacts (SQPC), examples of which are the S-2DEG-S junctions [3] and atomic contacts produced by break junctions [4, 5] and scanning tunneling microscope (STM) [6] techniques.

On the theoretical side there has also been a parallel advance with the development of fully quantum mechanical theories for the transport properties of superconducting one-channel contacts [7–10]. There has been a remarkable agreement between theoretical predictions and experimental results for the quantities that have so far been measured. These quantities include the phase-dependent supercurrent in a high transmissive contact [11] and the dc current at constant bias voltage [5, 6]. As we discuss in this paper, there remain many exciting predictions of the microscopic theories to be explored experimentally.

The aim of this paper is to present an overview of the main theoretical results that have been obtained for different microscopic models of an SQPC. An interesting aspect of superconducting transport is that qualitatively different behaviors are exhibited depending on how the system is biased. This will be analyzed in this work by discussing the cases of phase, voltage and current bias together with the case of transport

0749–6036/99/050925 + 12 $30.00/0

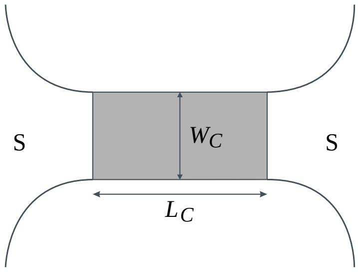

Fig. 1. Schematic representation of a superconducting quantum point contact.

under microwave radiation. The models are introduced in Section 2 together with the nonequilibrium Green's functions formalism used to calculate their transport properties. Section 3 is devoted to the voltage biased case for which we discuss the comparison of the fully quantum mechanical calculation with semiclassical standard theories and the available experimental results. We also discuss the limit of very small voltage. In Section 4 the current biased case is briefly analyzed, while the response under microwave radiation and its possible relevance for directly detecting Andreev states is discussed in Section 5. Thermal and shot-noise are the subject of Section 6 where we discuss the conditions for observing coherent transport of multiple charge quanta from the noise–current ratio. Finally, in Section 7, the superconducting transport through a resonant level is analyzed both in the limits of very large and very small charging energy. The general conclusions are summarized in Section 8.

2. Microscopic model and Green's function formalism

A schematical representation of a quantum point contact is depicted in Fig. 1. For a typical point contact the length of the constriction between the electrodes, L_c, is much smaller than the superconducting coherence length ξ_0 and its width W_c is $\sim \lambda_F$, the electron Fermi wavelength. The first condition ensures that the detailed superconducting phase and electrochemical potential profiles in the constriction region are unimportant and can be safely approximated by step functions. On the other hand, the condition $W_c \sim \lambda_F$ implies that there are only a few conduction channels between the electrodes.

The general mean-field Hamiltonian for a superconducting system can be written in terms of the electron field operators $\hat{\psi}_\sigma(\boldsymbol{r})$

$$\hat{H} = \int d\boldsymbol{r} \left\{ \sum_\sigma \hat{\psi}_\sigma^\dagger(\boldsymbol{r}) \mathcal{H}_e(\boldsymbol{r}) \hat{\psi}_\sigma(\boldsymbol{r}) + \Delta^*(\boldsymbol{r}) \hat{\psi}_\uparrow^\dagger(\boldsymbol{r}) \hat{\psi}_\downarrow^\dagger(\boldsymbol{r}) + \Delta(\boldsymbol{r}) \hat{\psi}_\downarrow(\boldsymbol{r}) \hat{\psi}_\uparrow(\boldsymbol{r}) \right\}, \tag{1}$$

where $\mathcal{H}_e$ is the one-electron Hamiltonian and $\Delta(\boldsymbol{r})$ is the superconducting order parameter. The problem of calculating transport properties in such a continuous representation for a nonhomogeneous system is extremely involved requiring the knowledge of the adequate boundary conditions at the interfaces. Some attempts in this direction have been recently presented by Zaitsev and Averin [12] within the quasiclasssical Green's functions approach. A different approach which circumvents these difficulties, while keeping a fully microscopic description of the problem, can be obtained by expanding the field operators in a discrete basis and writing the Hamiltonian (1) in the form [14]

$$\hat{H} = \sum_{i,\sigma} (\epsilon_i - \mu_i) c_{i\sigma}^\dagger c_{i\sigma} + \sum_{i \neq j, \sigma} t_{ij} c_{i\sigma}^\dagger c_{j\sigma} + \sum_i (\Delta_i^* c_{i\downarrow}^\dagger c_{i\uparrow}^\dagger + \Delta_i c_{i\uparrow} c_{i\downarrow}), \tag{2}$$

where i, j run over the different sites of the system, t_{ij} are the hopping parameters connecting the different sites; μ_i and Δ_i being the chemical potential and order parameter in a site representation. The simplification introduced by this approach allows us to deal with rather involved situations including spatial inhomogeneities (self-consistency) and nonstationary effects typically appearing in superconductors. For the voltage range eV $\sim \Delta$ the energy dependence of the transmission coefficients can be neglected and the transport properties can be expressed as a superposition of independent channels [13]. One can simplify the model even further to represent an SQPC with a single conduction channel, which can be described by the following Hamiltonian

$$\hat{H} = \hat{H}_L + \hat{H}_R + \sum_\sigma (te^{i\phi(\tau)/2} c^\dagger_{L\sigma} c_{R\sigma} + t^* e^{-i\phi(\tau)/2} c^\dagger_{R\sigma} c_{L\sigma}) - \mu_L \hat{N}_L - \mu_R \hat{N}_R, \tag{3}$$

where $H_{L,R}$ are the BCS Hamiltonians for the left and right uncoupled electrodes characterized by constant order parameters $\Delta_{L,R}$ (for a symmetric contact $\Delta_L = \Delta_R = \Delta$). $\phi(\tau)$ is the time-dependent superconducting phase difference entering as a phase factor in the hopping terms describing electron transfer between the electrodes. In our model the transmission, α, can be varied between 0 and 1 as a function of the coupling parameter t (see [8] for details). Within this model, the total current through the contact can be written as

$$I(\tau) = \frac{ie}{\hbar} \sum_\sigma (te^{i\phi(\tau)/2} \langle c^\dagger_{L\sigma}(\tau) c_{R\sigma}(\tau)\rangle - t^* e^{-i\phi(\tau)/2} \langle c^\dagger_{R\sigma}(\tau) c_{L\sigma}(\tau)\rangle). \tag{4}$$

The averaged quantities appearing in the current can be expressed in terms of nonequilibrium Green's functions [15]. For the description of the superconducting state it is useful to introduce spinor field operators (Nambu representation) [16], which in a site representation are defined as

$$\hat{\psi}_i = \begin{pmatrix} c_{i\uparrow} \\ c^\dagger_{i\downarrow} \end{pmatrix}, \quad \hat{\psi}^\dagger_i = (\, c^\dagger_{i\uparrow} \quad c_{i\downarrow}\,). \tag{5}$$

Then, the different correlation functions appearing in the Keldysh formalism adopt the standard causal form

$$\hat{G}^{\alpha,\beta}_{ij}(\tau_\alpha, \tau'_\beta) = -i\langle \hat{T}[\hat{\psi}_i(\tau_\alpha)\hat{\psi}^\dagger_i(\tau'_\beta)]\rangle, \tag{6}$$

where $\hat{T}$ is the chronological ordering operator along the closed time loop contour [15]. The labels α and β refer to the upper ($\alpha \equiv +$) and lower ($\alpha \equiv -$) branches on this contour. The functions $\hat{G}^{+-}_{ij}$, which can be associated within this formalism with the electronic nonequilibrium distribution functions [17], are given by the (2×2) matrix

$$\hat{G}^{+-}_{i,j}(\tau, \tau') = i \begin{pmatrix} \langle c^\dagger_{j\uparrow}(\tau') c_{i\uparrow}(\tau)\rangle & \langle c_{j\downarrow}(\tau') c_{i\uparrow}(\tau)\rangle \\ \langle c^\dagger_{j\uparrow}(\tau') c^\dagger_{i\downarrow}(\tau)\rangle & \langle c_{j\downarrow}(\tau') c^\dagger_{i\downarrow}(\tau)\rangle \end{pmatrix}. \tag{7}$$

In terms of the $\hat{G}^{+-}$, the current is given by

$$I(\tau) = \frac{e}{\hbar} Tr[\hat{\sigma}_z(\hat{t}\hat{G}^{+-}_{RL}(\tau,\tau) - \hat{t}^\dagger \hat{G}^{+-}_{LR}(\tau,\tau))], \tag{8}$$

where $\hat{t}$ is the hopping element in the Nambu representation

$$\hat{t} = \begin{pmatrix} t & 0 \\ 0 & -t^* \end{pmatrix}. \tag{9}$$

The Green's functions $\hat{G}^{+-}_{ij}$ are calculated using an infinite order perturbation theory with the coupling term in eqn (3) considered as a perturbation. Within this approach these Green's functions obey a set of integral Dyson equations [8]. As discussed in the next sections, the solution is strongly dependent on the biasing condition which determines the time dependence in the superconducting phase difference.

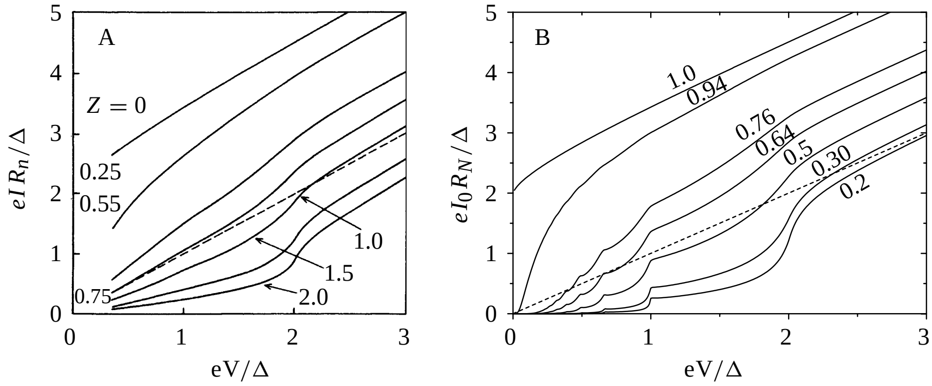

Fig. 2. dc current–voltage characteristics of a SQPC for different values of the normal transmission. Left panel corresponds to the semiclassical OTBK theory and right panel to the fully quantum mechanical calculation.

3. Current in a voltage biased contact

The simplest biasing condition is that of a constant applied voltage. This situation is rather easy to achieve experimentally except for very small voltages (see Section 4). In spite of its apparent simplicity, the theoretical analysis is quite complex because of the time-dependent phase difference which gives rise to a time-dependent current containing all harmonics of the Josephson frequency $\omega_0 = 2\mathrm{eV}/\hbar$, i.e. $I(\tau) = \sum_n I_n(V) \exp in\omega_0$. The current can be also decomposed into dissipative and nondissipative parts according to the different symmetry with respect to V of even and odd terms in the previous expansion [8].

In this case, the integral Dyson equations can be transformed into a set of algebraic equations by a double Fourier transformation defined by

$$\hat{G}_{n,m}(\omega) = \int d\tau \int d\tau' e^{-i\omega_0(n\tau - m\tau')/2} e^{i\omega(\tau-\tau')} \hat{G}(\tau, \tau'). \tag{10}$$

An efficient algorithm for the numerical evaluation of the Green's function Fourier components is discussed in Ref. [8].

In this section, we shall concentrate on the dc component of the current I_0 which is the quantity more readily accessible experimentally. Figure 2 shows the dc I–V characteristics calculated from the fully quantum mechanical theory and from the semiclassical OBTK theory [18]. As can be observed, the results become increasingly different for decreasing transmission. The fully quantum-mechanical calculation exhibits a pronounced subgap structure with steps at $\mathrm{eV} = 2\Delta/n$ which is hardly noticeable in the semiclassical theory. Both theories give the same result, nevertheless, for perfect transmission where interference effects, not included in the semiclassical theory, disappear due to the absence of backscattering.

The experimental I–V characteristics for atomic contacts of different metals are in remarkable agreement with our theoretical results. This is illustrated in Fig. 3 for the case of a one-atom contact made of Pb (these results are taken from Ref. [6]). This agreement makes it possible to extract information on the conduction channels transmissions T_n of metallic atomic contacts [5, 6, 19].

The temperature dependence of the I–V characteristics is shown in Fig. 4 for different values of transmission. A remarkable feature of this dependence is that the SGS persists up to temperatures close to the critical temperature. When normalized to the temperature-dependent superconducting gap, the dc current exhibits a certain increase at low transmission, the opposite behavior being found close to prefect transmission. The crossover between these two tendencies is found for $\alpha \sim 0.8$.

The limit of very small bias is particularly interesting due to the contribution of MAR processes of

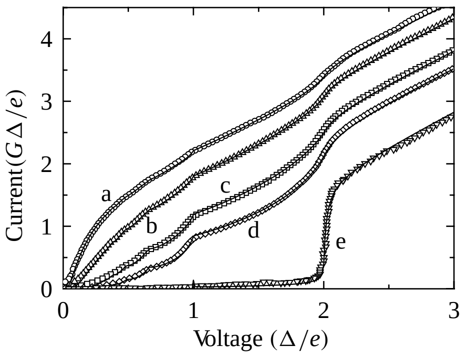

Fig. 3. Measured current–voltage characteristics (symbols) for different realizations of a Pb one-atom contact at 1.5 K fabricated with the STM technique [6]. The full lines are numerical fits obtained by superposing four one-channel I–V curves with different transmissions.

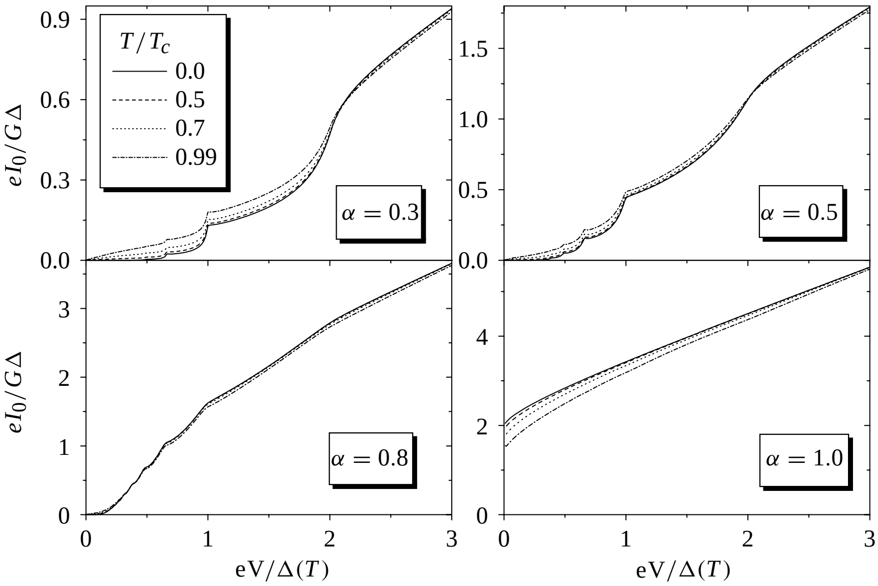

Fig. 4. dc current–voltage characteristic for different temperatures and four values of the transmission.

increasing order $n \sim 2\Delta/\mathrm{eV}$. This divergency in the $V \to 0$ limit is eventually controlled by the presence of an inelastic relaxation rate η (usually a small fraction of the gap parameter) which introduces a cut-off in the theory when $\mathrm{eV} < \eta$. The effect of the inelastic relaxation rate is to damp MAR processes of order $n > 2\Delta/\eta$. As a consequence, the system experiences a transition into a different regime where the total current becomes linear in V. In this regime, the system response is determined by the adiabatic dynamics of the Andreev states at $\epsilon(\phi) = \Delta\sqrt{1 - T\sin^2(\phi/2)}$ which move following the actual value of the superconducting phase. The total current can then be written as $I(\phi, V) = I_S(\phi) + G(\phi)V$ [20], where the supercurrent $I_S(\phi)$ and the phase-dependent linear conductance $G(\phi)$ are given by

$$I_S(\phi) = \frac{e\Delta}{2\hbar}\frac{\alpha\sin\phi}{\sqrt{1 - \alpha\sin^2(\phi/2)}}\tanh\left(\frac{\beta\epsilon(\phi)}{2}\right)$$

$$G(\phi) = \frac{2e^2}{h}\frac{\pi}{16\eta}\left[\frac{\Delta\alpha\sin\phi}{\sqrt{1-\alpha\sin^2(\phi/2)}}\mathrm{sech}(\frac{\beta\epsilon(\phi)}{2})\right]^2\beta V. \tag{11}$$

The expression of the supercurrent [14, 21, 22] in eqn (11) interpolates between the Josephson $I_S \sim \sin\phi$ behavior and the Kulik–Omelyanchuk $I_S \sim \sin\phi/2$ ballistic limit [23]. This behavior at high transmission has been recently confirmed experimentally using break junction techniques in an SQUID configuration [11]. It should be noted that the expression for $G(\phi)$ gives a definite answer to an old-standing problem concerning the form of this term known as the '$\cos\phi$ problem' [24]. The precise form of this term remains to be explored experimentally (a similar set-up to that used in Ref. [11] could be used for this purpose).

Finally, it should be stressed that, from a mathematically point of view, the two limits $\eta \to 0$ and $V \to 0$ are not interchangeable [8]. In practice, the limit eV $\to 0$ with eV $> \eta$ can never be reached as there is always a finite, although small, inelastic relaxation rate present.

4. Current biased contact

At very low voltages (and specially for high transmission), the contact impedance may become actually smaller than the voltage source impedance. If these conditions apply, the assumption of having an ideal source providing a constant voltage bias which fixes the phase dynamics is no longer valid. In this case one should take into account the electromagnetic environment of the contact in order to determine the phase dynamics and the system response to the external bias.

For conventional tunnel junctions this limit is usually analyzed by means of the RSJ and RSCJ models [2, 24] which represent the actual environment by a simple shunted circuit with a resistance R and a capacitance C connected in parallel to the junction. Within these simple models the phase dynamics are equivalent to that of a particle moving in a 'tilted washboard' potential $U(\phi) = -I_b\phi + I_c\cos\phi$, where I_b is the biasing current and I_c is the Josephson critical current. At finite temperatures one should also consider thermal fluctuations acting as an stochastic force on the fictitious particle.

To analyze the response of an SQPC under current bias one should generalize these models for contacts of arbitrary transmission [25]. The description of the superconducting phase as a classical variable will be valid as long as the Josephson coupling energy $E_J \sim \hbar I_c/2e$ is much larger than the charging energy $E_c \sim e^2/2C$. For an SQPC connected to a current source, the equations for the generalized RSCJ model would be given by

$$\begin{aligned} I_b &= \frac{\hbar}{2e}C\ddot{\phi} + \frac{\hbar}{2e}G(\phi)\dot{\phi} + I_S(\phi) + i_n(\phi) \\ V &= \frac{\hbar}{2e}\dot{\phi}, \end{aligned} \tag{12}$$

where $I_S(\phi)$ and $G(\phi)$ are given by eqn (11) of the previous section and $i_n(\phi)$ is a fluctuating current whose power spectrum S is related to $G(\phi)$ by the fluctuation-dissipation theorem $S = 4k_BTG$ (see Section 6). It should be noted that the above equations are strictly valid in the limit of small voltages induced on the contact, i.e. eV $< \eta$, which is the condition for the validity of eqn (11) in Section 3. The actual value of η is unknown but can be estimated to be of the order of $\Delta/100$ or less.† In the mechanical analogy, the effective potential for the generalized RSCJ model can be written as

$$U(\phi) = -\left\{I_b\phi + \frac{4e}{\beta\hbar}\log\left[\cosh\left(\frac{\beta\epsilon(\phi)}{2}\right)\right]\right\} \tag{13}$$

and there appears a 'position'-dependent friction which comes from the dissipative term in $G(\phi)$. The

†This small value is consistent with the agreement between theory and experiments in the constant voltage case.

inclusion of this phase-dependent term should have important consequences in the dynamics of the system. Note that the particular form of $G(\phi)$ (eqn (11)) introduces a very asymmetrical friction with a minimum at the local minima of $U(\phi)$ and maximum at the local maxima.

Integrating eqn (12) for the generalized RSCJ model under arbitrary conditions is a formidable task. An approximate solution for the overdamped case, i.e. $G(\phi)/C > (2eI_c/\hbar C)^{1/2}$, can be obtained following the procedure introduced by Ambegaokar and Halperin [26] for overdamped tunnel junctions. The generalization of the Ambegaokar and Halperin theory is straightforward once we had identified the generalized potential (eqn (13)) and the shunted resistance with $1/G(\phi)$ (details will be given elsewhere). The measurement of the slope of the I–V curve at zero voltage, which is directly related to $G(\phi)$, would provide information on the value of η in real systems.

5. Contact under microwave radiation

As discussed in Section 3, the Andreev states play a central role in determining the adiabatic dynamics of an SQPC at low bias voltage. Considering that typical subgap energies are in the microwave range, it seems natural to propose using microwave radiation for a direct detection of Andreev states. This possibility has been suggested in a previous work by us [27] and in Ref. [28].

The effect of a microwave external field can be easily introduced in the single-channel contact model. One can assume that the field intensity is maximum in the constriction region and neglect the effect of the field penetrating inside the electrodes. Within this assumptions the field can be introduced as a phase factor modulating the hopping term t in eqn (3), i.e.

$$t(\tau) = te^{i\alpha_0 \cos \omega_r \tau}, \tag{14}$$

where ω_r is the microwave frequency, $\alpha_0 = \mathrm{eV}_{opt}/(\hbar\omega_r)$, V_{opt} being the optical voltage induced by the field across the constriction. The parameter α_0 measures the strength of the coupling with the external field. The time-dependent hopping term can be expanded as

$$t(\tau) = t \sum_n i^n J_n(\alpha_0) e^{in\omega_r \tau}, \tag{15}$$

where J_n is the n-order Bessel function. For small coupling one can keep the lowest order terms in eqn (15) and obtain some analytical results [27]. In the general case, the model Hamiltonian can be viewed, according to eqn (15), as a superposition of processes where an arbitrary number of quanta of energy $\hbar\omega_r$ are absorbed or emitted. As the temporal dependence of each term in eqn (15) is formally equivalent to that in the constant voltage case, the generalization of the algorithm discussed in Section 3 to the present case is straightforward.

Figure 5 shows the induced dc current as a function of microwave frequency for the case of a low coupling constant ($\alpha_0 = 0.1$). All these results correspond to the situation in which the contact is carrying the maximum supercurrent. In this weak coupling limit the induced current is mainly due to the excitation from the lower to the upper Andreev state, which carries a negative current (i.e. opposite to the supercurrent). As a consequence, the induced current exhibits a maximum for the resonant condition $\omega_r = 2\epsilon(\phi)$. At resonance, the induced current can be of the same order as the critical supercurrent. One can also notice a second stellite peak around $\epsilon(\phi)$ associated with *two photon* processes and a continuous band above $\Delta + \epsilon(\phi)$. When the coupling constant α_0 increases, the contribution of higher order processes becomes progressively more important giving rise to a complex structure where the resonant condition for the excitation of the upper Andreev state can no longer be resolved [27].

6. Thermal and shot-noise

The analysis of current fluctuations has a central role in the theory of transport in mesoscopic systems [29]. Fluctuations can provide useful information on the microscopic dynamics (correlations) not contained in the

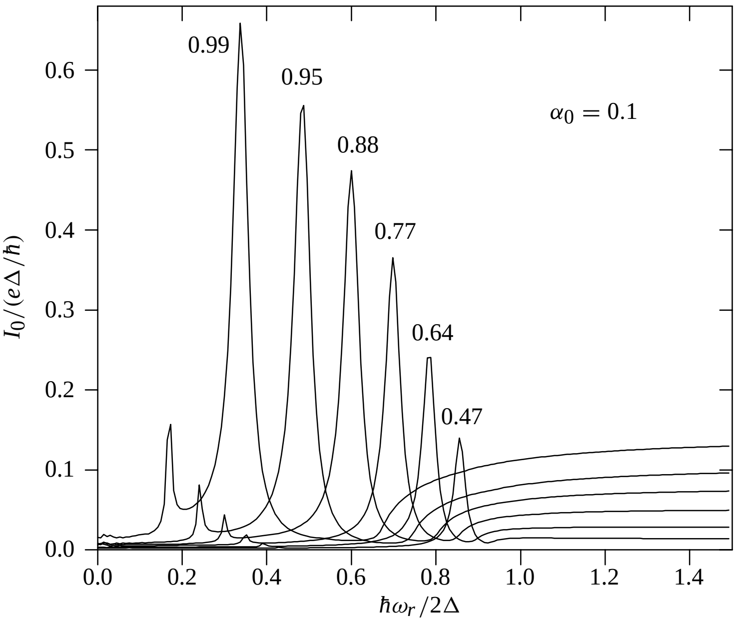

Fig. 5. Induced dc current in a SQPC under microwave-radiation for different values of the transmission. The parameter α_0 controls the coupling to the external field (see text).

average current. It is thus desirable to develop a fully quantum-mechanical theory of current fluctuations in an SQPC on an equal footing as previously discussed for the current. In this respect, some limiting cases have already been analyzed in the recent literature: the excess noise for eV $\gg \Delta$ in a ballistic contact has been discussed in Ref. [30], thermal noise for arbitrary transmission was analyzed in Ref. [31] while the case of perfect transmission and finite voltages has been addressed in Ref. [32].

The noise power spectrum is defined by

$$S(\omega, \tau) = \hbar \int d\tau' e^{iw\tau'} \langle \delta\hat{I}(\tau + \tau')\delta\hat{I}(\tau) + \delta\hat{I}(\tau)\delta\hat{I}(\tau + \tau')\rangle, \tag{16}$$

where $\delta\hat{I}(\tau) = \hat{I}(\tau) - \langle\hat{I}(\tau)\rangle$. For the evaluation of the above correlation functions a BCS mean-field decoupling procedure can be performed. $S(\omega, \tau)$ can then be written in terms of nonequilibrium Green's functions introduced in Section 3. In the voltage biased case, $S(\omega, \tau)$ can be expanded in harmonics of the Josephson frequency, i.e. $S(\omega, \tau) = \sum S_n(\omega) \exp in\omega_0\tau$. As in the case of the average current, the noise Fourier components $S_n(\omega)$ can be evaluated in terms of the Green's functions matrix elements $G_{n,m}$ defined in Section 3.

Let us start by analyzing the $V = 0$ case where noise is due to thermal fluctuations. While in a normal QPC thermal noise has the usual well understood behavior, increasing linearly with temperature and with a flat frequency spectrum, in the superconducting case it exhibits very unusual behavior as a function of temperature, frequency and phase. Figure 6 illustrates the frequency dependence of the thermal noise for different transmissions. As can be observed, the noise exhibits two sharp resonances at $\omega = 0$ and $\omega = 2\epsilon(\phi)$ corresponding to the excitation of the Andreev bound states. For $\omega > \Delta + |\epsilon(\phi)|$, S exhibits a broad band arising from the continuous part of the single particle spectral density.

The weight of the peaks at 0 and $2\epsilon(\phi)$ can be evaluated analytically as discussed in Ref. [31]. We find that the zero frequency noise is related to the phase-dependent linear conductance by $S(0) = 4k_BTG(\phi)$

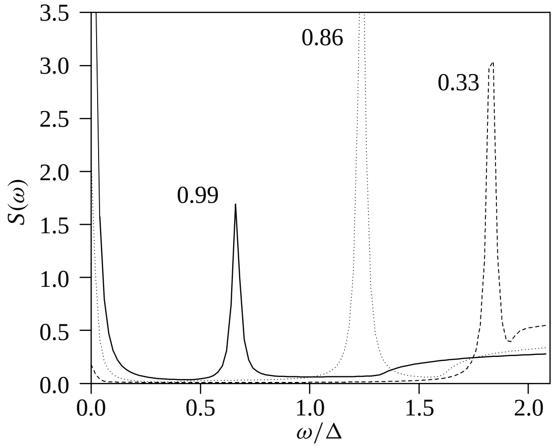

Fig. 6. Power spectrum $S(\omega)$ of the zero–voltage current-fluctuations at $k_B T = 0.2\Delta$ in a SQPC for three transmission values. The contact is biased at the maximum supercurrent.

as expected from the fluctuation dissipation theorem. The exponential temperature dependence in $G(\phi)$ gives rise to an exponential increase of thermal noise when $k_B T \sim \epsilon(\phi)$. It should be noted that the ratio $S(0)/2eI_S(\phi)$ can actually be divergent for any temperature provided that $\alpha \to 1$ and $\phi \to \pi$. On the other hand, the weight of the peak at $2\epsilon(\phi)$ is zero for perfect transmission, increasing as $\alpha^2(1-\alpha)$, becoming the dominant feature for finite $1-\alpha$ and sufficiently low temperatures. In fact, the ratio between $S(2\epsilon(\phi))$ and $S(0)$ is given by

$$S(2\epsilon(\phi))/S(0) = \frac{1}{2}(1-\alpha)\tan^2\frac{\phi}{2}\cosh\left[\frac{\epsilon(\phi)}{k_B T}\right]. \quad (17)$$

Another quantity which is interesting to analyze and is directly amenable to experimental measurement is the shot-noise. Mathematically the shot-noise is given by the zero frequency dc component in the expansion of the noise power spectrum, i.e. $S_0(0)$, at eV $\gg k_B T$. For simplicity we will consider the zero temperature case. Results for the shot-noise as a function of voltage are shown in Fig. 7 for several transmissions. The curves exhibit a pronounced subgap structure at the voltage values eV $= 2\Delta/n$ as in the dc current. In the case of the shot-noise, the structure is more pronounced and is still observable for transmissions rather close to 1. In the perfect ballistic limit, shot-noise is greatly reduced due to correlations associated with the Pauli principle as in the case of a normal ballistic contact [33].

On the other hand, in the tunnel limit the shot-noise is expected to reach the Poisson limit $S \sim 2qI$, where q is the transmitted charge in an elementary process. This relation offers the possibility to directly check whether multiple charges $q = ne$ are actually being transmitted coherently in a nth order MAR process [34]. Our theory allows one to calculate the effective charges defined by the shot-noise current ratio. In the tunnel limit one finds that q exhibits a well-defined step-like behavior $q/e = 1 + Int[2\Delta/\text{eV}]$ confirming the above hypothesis [35].

7. SGS and resonant tunneling

The model discussed so far describes an SQPC with an energy-independent transmission α. In some situations, that can be achieved experimentally, the normal transmission can have a nonnegligible variation on an energy scale of the order of Δ. This can happen when the constriction region is weakly coupled to the electrodes by tunnel barriers as in the case of a small metallic particle or a quantum dot coupled to

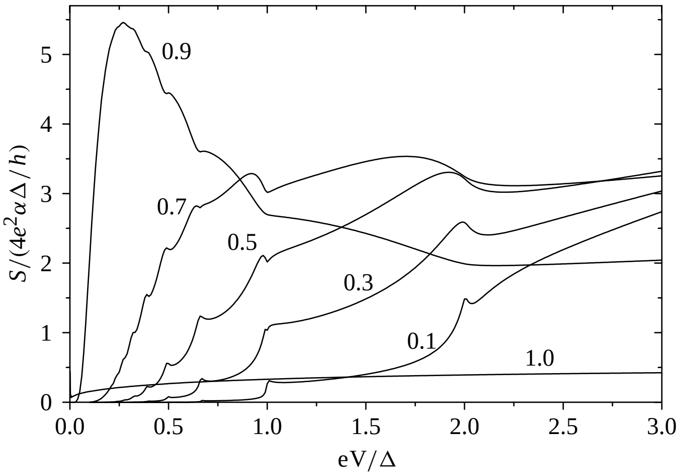

Fig. 7. Zero-frequency current-fluctuations at zero temperature (shot-noise) as a function of bias voltage.

superconducting leads [36]. We represent this situation by the following model Hamiltonian

$$\hat{H} = \hat{H}_L + \hat{H}_R + \sum_{\nu,\sigma} t_\nu(\hat{c}^\dagger_{\nu\sigma}\hat{c}_{0\sigma} + \hat{c}^\dagger_{0\sigma}\hat{c}_{\nu\sigma}) + \sum_\sigma \epsilon_0 \hat{n}_{0\sigma} + U\hat{n}_{0\uparrow}\hat{n}_{0\downarrow}, \quad (18)$$

where $\hat{H}_L$ and $\hat{H}_R$ describe the left and right leads, ϵ_0 is a resonant level associated with the isolated constriction region, t_ν with $\nu = L, R$ are hopping parameters which connect the level to the left and right leads. The U term takes into account the Coulomb repulsion in the constriction region. The parameter U is basically the charging energy, E_c, and is related to the central region capacitance C by $U \sim e^2/2C$. For the subsequent discussion it is convenient to introduce the normal elastic tunneling rates $\Gamma_\nu = \pi|t_\nu|^2\rho_\nu(\mu)$, where $\rho_\nu(\mu)$ are the normal spectral densities of the leads at the Fermi level.

When the charging energy is much larger than both Γ and Δ, Andreev reflections are completely suppressed and transport is only due to single-quasiparticle tunneling. This situation has been achieved in experiments on transport through nanometer metallic particles by Ralph *et al.* [36]. Model calculations presented by us in Ref. [37] based on the Hamiltonian given in eqn (18) yield good agreement with the experimental results.

We shall consider in more detail the case of small charging energy, in which the interplay between resonant tunneling and MAR gives rise to novel effects and a very rich subgap structure [37, 38]. Figure 8 shows the dc I–V characteristic for different positions of the resonant level ϵ_0 with respect to the Fermi level. The tunneling rates are taken in this case as $\Gamma_L = \Gamma_R = \Delta$. As can be observed, when the level is far from the gap region (case a) the limit of energy-independent transmission is recovered and the subgap structure is similar to the one depicted in Fig. 2 (right panel). As the resonant level approaches the gap region, the subgap structure becomes progressively distorted with respect to the energy-independent transmission case. While the structure corresponding to the opening of odd-order MAR processes (i.e. at eV $\sim 2\Delta/n$ with odd n) is enhanced, the structure at eV $\sim 2\Delta/n$ with even n is suppressed. When $\Gamma \to 0$ (not shown), one can also note the appearance of resonant peaks in the I–V characteristic for eV $\sim 2\epsilon_0$.

8. Conclusions

An overview of the results of a microscopic theory for the transport properties of superconducting quantum point contacts has been presented. These results include the response under different biasing conditions for

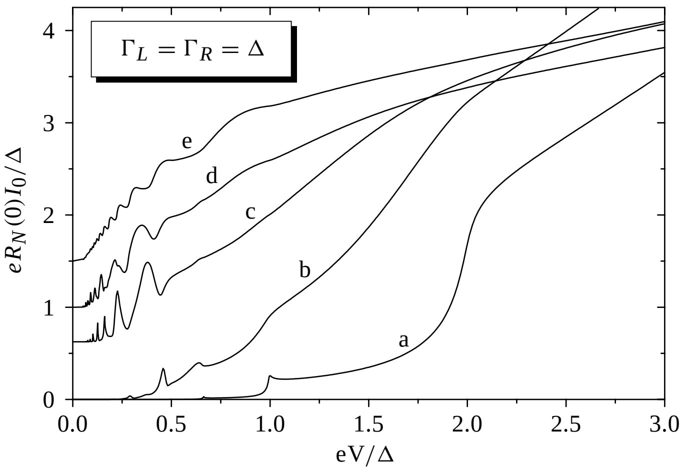

Fig. 8. dc current–voltage characteristic for a resonant level ϵ_0 coupled to superconducting leads. $\epsilon_0 = 5\Delta$ (a), 2Δ (b), Δ (c), $\Delta/2$ (d) and 0 (e). $R_N(0)$ is the normal resistance at the Fermi level. Curves (c), (d) and (e) have been displaced for the sake of clarity.

an energy-independent transmission as well as the case of resonant transmission. A remarkable agreement has been found between the calculated and the experimental dc I–V curves for atomic-size contacts [5, 6]. The agreement has allowed us to extract information on the number and transmissions of the conduction channels in atomic contacts of different metallic elements [6, 19]. On the other hand, the agreement shows the importance of interference effects included in a fully quantum-mechanical calculation and thus the need to go beyond semiclassical theories for describing these kind of systems. Additional predictions of the microscopic theory remain to be analyzed experimentally. For instance, we could point out the phase dependence of the linear conductance, the direct observation of Andreev levels in contacts under microwave radiation and the analysis of shot-noise. This last analysis would provide direct evidence of coherent transmission of multiple charges in MAR processes. Finally, the rich SGS in the presence of resonant transmission could be explored in S-2DEG-S devices which are currently being developed [3].

Acknowledgements—The authors would like to thank C. Urbina for fruitful discussions. This work has been supported by the Spanish CICyT under contract PB97-0044.

References

[1] B. D. Josephson, Phys. Lett. **1**, 251 (1962).
[2] M. Tinkham, *Introduction to Superconductivity* (McGraw-Hill, New York, 1996).
[3] H. Takayanagi, T. Akazaki, and J. Nitta, Phys. Rev. Lett. **75**, 3533 (1995).
[4] N. van der Post, E. T. Peters, I. K. Yanson, and J. M. van Ruitenbeek, Phys. Rev. Lett. **73**, 2611 (1994).
[5] E. Scheer, P. Joyez, D. Esteve, C. Urbina, and M. H. Devoret, Phys. Rev. Lett. **78**, 3535 (1997).
[6] E. Scheer, N. Agraït, J. C. Cuevas, A. Levy Yeyati, B. Ludolph, A. Martin-Rodero, G. Rubio, J. M. van Ruitenbeek, and C. Urbina, Nature **394**, 154 (1998).
[7] D. Averin and A. Bardas, Phys. Rev. Lett. **75**, 1831 (1995).
[8] J. C. Cuevas, A. Martin-Rodero, and A. Levy Yeyati, Phys. Rev. **B54**, 7366 (1996).
[9] M. Hurd, S. Datta, and P. F. Bagwell, Phys. Rev. **B54**, 6557 (1996).
[10] E. N. Bratus, V. S. Shumeiko, E. V. Bezuglyi, and G. Wendin, Phys. Rev. **B55**, 1266 (1997).
[11] M. C. Koops, G. V. van Duyneveldt, and R. de Bruyn Ouboter, Phys. Rev. Lett. **77**, 2524 (1996).
[12] A. V. Zaitsev and D. V. Averin, Phys. Rev. Lett. **80**, 3602 (1998).

[13] C. J. W. Beenakker, Phys. Rev. **B46**, 12841 (1992).
[14] A. Martin-Rodero, F. J. Garcia-Vidal, and A. Levy Yeyati, Phys. Rev. Lett. **72**, 554 (1994); Surf. Sci. **307–309**, 973 (1994); A. Levy Yeyati, A. Martin-Rodero, and F. J. Garcia-Vidal, Phys. Rev. **B51**, 3743 (1995).
[15] L. V. Keldish, Zh. Eksp. Teor. Fiz. **47**, 1515 (1964) [Sov. Phys. JETP **20**, 1018 (1965)].
[16] Y. Nambu, Phys. Rev. **117**, 648 (1960).
[17] L. P. Kadanoff and G. Baym, *Quantum Statistical Mechanics* (Benjamin, New York, 1962).
[18] T. M. Klapwijk, G. E. Blonder, and M. Tinkham, Physica **B109–110**, 1657 (1982); M. Octavio, M. Tinkham, G. E. Blonder, and T. M. Klapwijk, Phys. Rev. **B27**, 6739 (1983); K. Flensberg, J. B. Hansen, and M. Octavio, Phys. Rev. **B38**, 8707 (1988).
[19] J. C. Cuevas, A. Levy Yeyati, and A. Martin-Rodero, Phys. Rev. Lett. **80**, 1066 (1998).
[20] A. Martin-Rodero, A. Levy Yeyati, and J. C. Cuevas, Physica **B218**, 126 (1996); A. Levy Yeyati, A. Martin-Rodero, and J. C. Cuevas, J. Phys.: Condens. Matter **8**, 449 (1996).
[21] W. Haberkorn, H. Knauer, and J. Richter, Phys. Status Solidi **47**, K161 (1978).
[22] C. W. J. Beenakker, Phys. Rev. Lett. **67**, 3836 (1991).
[23] O. Kulik and N. Omel'yanchuk, Fiz. Nizk. Temp. **3**, 945 (1977); O. Kulik and N. Omel'yanchuk, **4**, 296 (1978) [Sov. J. Low Temp. Phys. **3**, 459 (1997); **4**, 142 (1998)].
[24] A. Barone and G. Paterno, *Physics and Applications of the Josephson Effect* (Wiley, New York, 1982).
[25] The case of perfect transmission has been recently discussed in D. V. Averin, A. Bardas, and H. T. Iman, Phys. Rev. **B58**, 11165 (1998).
[26] V. Ambagaokar and B. J. Halperin, Phys. Rev. Lett. **22**, 1364 (1969).
[27] A. Levy Yeyati, J. C. Cuevas, and A. Martin-Rodero, *Photons and Local Probes*, edited by O. Marti and R. Müller (Kluwer Academic, Dordrecht, 1995).
[28] V. S. Shumeiko, G. Wendin, and E. N. Bratus, Phys. Rev. **B48**, 13129 (1993).
[29] For a recent review, see M. J. M. de Jong and C. W. J. Beenakker, *Mesoscopic Electron Transport*, NATO ASI Series E Vol. 345, edited by L. L. Sohn, L. P. Kouwenhoven, and G. Schön (Kluwer Academic Publishing, Dordrecht, 1997).
[30] J. P. Hessling, V. S. Shumeiko, Yu. M. Galperin, and G. Wendin, Europhys. Lett. **34**, 49 (1996).
[31] A. Martin-Rodero, A. Levy Yeyati, and F. J. Garcia-Vidal, Phys. Rev. **B53**, R8891 (1996).
[32] D. V. Averin and H. T. Imam, Phys. Rev. Lett. **76**, 3814 (1996).
[33] V. A. Khlus, Sov. Phys. JETP **66**, 1243 (1987).
[34] P. Dieleman, H. G. Bukkems, T. M. Klapwijk, M. Schicke, and K. H. Gundlach, Phys. Rev. Lett. **79**, 3486 (1997).
[35] J. C. Cuevas, A. Martin-Rodero, and A. Levy Yeyati, Phys. Rev. Lett. **82**, 4086 (1999).
[36] D. C. Ralph, C. T. Black, and M. Tinkham, Phys. Rev. Lett. **74**, 3241 (1995).
[37] A. Levy Yeyati, J. C. Cuevas, A. López-Dávalos, and A. Martin-Rodero, Phys. Rev. **B55**, R6137 (1997).
[38] G. Johansson, V. S. Shumeiko, E. N. Bratus, and G. Wendin, Physica **C293**, 77 (1997).